Chemical Bath Deposition of Cu_2O Thin Films on FTO Substrates: Effect of Sequential Deposition.

Odín Reyes-Vallejo
Sección de Electrónica de Estado Sólido- Ingeniería eléctrica (SEES), CINVESTAV- IPN, Ciudad de México, México
odin.reyes.v@cinvestav.mx

Rocío M. Sánchez-Albores
Escuela de Ciencias Químicas, Universidad Autónoma de Chiapas (UNACH), Chiapas, México
magdalena.sanchez@unach.mx

Arturo Fernández-Madrigal
Instituto de Energías Renovables-UNAM (IER-UNAM), Morelos, México
afm@ier.unam.mx

Francisco J. Cano
Programa de Nanociencia y nanotecnología, CINVESTAV- IPN, Ciudad de México, México
franciscojavier.cano@cinvestav.edu.mx

C.A. Meza-Avendaño
Instituto de Investigación e Innovación en Energías Renovables (IIIER-UNICACH), Chiapas, México
carlos.meza@unicach.mx

J.J. Díaz
Programa de Nanociencia y nanotecnología, CINVESTAV- IPN, Ciudad de México, México
jose.diaz@cinvestav.mx

A. Ashok
Sección de Electrónica de Estado Sólido- Ingeniería eléctrica (SEES), CINVESTAV- IPN, Ciudad de México, México
ashokad@cinvestav.mx

P. J. Sebastian
Instituto de Energías Renovables-UNAM (IER-UNAM), Morelos, México
sjp@ier.unam.mx

ABSTRACT:
*Sequential deposition of Cu_2O on FTO substrates was performed by chemical bath deposition to increase the thickness of the films. The variation of structural, optical, morphological, and electrochemical properties was studied as the number of deposits increased. The increase of thickness promotes an increase in the crystallite size and the lattice constant **a**, as well as a shift in the region of the absorption of light towards lower energies, reducing the band gap and the transmittance slightly. Also, it was estimated a change in the preferential orientation from the plane (111) to (200), caused a decrease in the structural disorder (Urbach energy) as a consequence of reducing the conductivity. On the other hand, during the electrochemical characterization a p-type behavior was observed in all the films, and as the thickness increased a shift towards more positive flat band potential values and a decrease in the carrier concentration was observed, which is the result of the decrease in structural disorder. The photocurrent measurements showed that the best performances were by the thinnest and the thickest films because some are the most conductive and the others absorb more light.*

Keywords— *Cuprous oxide, chemical bath deposition, sequential deposition, photoelectrochemical cell, and thickness increase effect.*

I INTRODUCTION:

Cuprous oxide is a very attractive material because it is formed by abundant, not toxic, and low-cost materials. But also, presents outstanding optoelectronic properties with a tunable band gap from 1.9 to 2.7 eV, great absorption coefficient ($>10^5$ cm^{-1}), high hole mobility, and tunable conductivity in a wide range [1-3]. Structural defects are essential for the electrical behavior of Cu_2O films, being the Cu vacancies the mainly responsible for its p-type nature [4]. Therefore, it is essential to know the structural disorder in the film to explain its electrical properties.

It can be used as thin film or as particles in diverse solar harvesting applications like solar cells, photoelectrochemical cells, and photocatalysis [5-7]. These thin films can be deposited by physical and chemical methods such as sputtering, evaporation, annealing of Cu foils, electrodeposition, and spray pyrolysis [5,8-11]. The chemical bath deposition (CBD) is an easy, simple, and reproducible method for thin films deposition, in previous studies, we have reported the deposition of Cu_2O by CBD using a very thin film of Cu_xS before the Cu_2O deposition to promote adherence but also triethanolamine to control the rate deposition [12]. The fast precipitation of Cu_2O in an aqueous solution limits the growth of the films, according to some reports the maximum thickness achieved was from 100 to 500 nm [13,14] reporting peeling problems, in our case we have deposited up to 900 nm on corning glass [3].

In the present study, we present sequential CBD to increase the thickness of Cu_2O thin films deposited in FTO substrates to enhance light absorption and develop films suitable for solar and photoelectrochemical purposes, since more than 1 µm is needed for correct light absorption. FTO (Fluorine-doped Tin Oxide) was selected since it is a transparent conductive metal oxide used as a transparent electrode for thin film photovoltaics.

978-1-6654-5508-4/22/$31.00 ©2022 IEEE

II EXPERIMENTAL:

Before the Cu_2O thin films, 30 nm of Cu_xS was deposited as we have described previously [12]. $CuSO_4$, $Na_3C_6H_5O_7$, $C_6H_{12}O_6$, and NaOH were used as the copper source, complexing, reducing, and oxidizing agents, respectively, preparing a 1M solution of each reactant. 30, 22.5 and 20 ml of $CuSO_4$, $Na_3C_6H_5O_7$, and $C_6H_{12}O_6$ solutions were mixed for 5 minutes, then 15 ml of triethanolamine (TEA) concentrated was added to increase the complexing grade. The pH was adjusted to 9.5 with NaOH solution and water is added to complete the solution up to 100 ml. Then, the FTO substrates with the Cu_xS deposited were immersed in the solution with the conductive film towards the wall of the recipient. The deposition was performed at 70ºC for 4 hours, and finally, the films were washed with water and cotton to remove the material not well adhered to and ensure the growth of the next deposit (No damage to the films was observed because of the use of cotton). For sequential depositions, the process was repeated up to 4 times. The thin films were labeled 1D, 2D, 3D, and 4D concerning the deposit number.

III CHARACTERIZATION:

X-ray diffraction was used to identify the phases of the samples using a Rigaku diffractometer under Cu-Kα radiation (λ=1.5406 Å) in the 2θ range of 20–70º (2°/min).
The preferential orientation was calculated through the texture coefficients equation (1)

$$T_{c(hkl)} = \frac{\frac{I_{i(hkl)}}{I_{o(hkl)}}}{\frac{1}{n}*\sum_{i=1}^{n}\frac{I_{i(hkl)}}{I_{o(hkl)}}} \qquad 1$$

where, h,k, and l are the Miller indices, $I_{(hkl)}$ and $I_{O(hkl)}$ are the intensities of the planes (hkl) of the sample and the pattern, and n is the number of planes considered in the analysis. The structural characterization was done by calculating the crystallite size D and lattice constant *a* (in the cubic system *a* = *b* = *c*), using equations 2 and 3 respectively:

$$D = \frac{\kappa*\lambda}{b*\cos\theta} \qquad 2$$

$$d_{hkl} = \frac{a}{\sqrt{h^2+k^2+l^2}} \qquad 3$$

where d_{hkl} is the interplanar spacing of the plane (hkl), θ is the Bragg's angle, b is the full-width at half-maximum (FWHM) of the peak (in radians), and k is a constant of value 0.9.

An Ambios Profiler (XP-200) was used to measure the thickness of the films. The surface morphology was analyzed by field emission scanning electron microscopy (FE-SEM) using a Hitachi FE-SEM S-5500. UV-VIS spectroscopy in the spectral range of 400 to 1500 nm was performed using a JASCO spectrophotometer (V-670) to estimate the optical parameters. The absorption coefficient was calculated by taking into consideration equation 4.

$$\alpha(\lambda) = \frac{1}{t}ln\left[\frac{(1-R)^2}{2T} + \sqrt{\frac{(1-R)^4}{4T^2} + R^2}\right] \qquad 4$$

where T and R are the corrected transmittance and reflectance, t is the thickness of the film and $\alpha(\lambda)$ is the absorption coefficient at wavelength λ. The band gap (Eg) was calculated by equation 5.

$$\alpha hv = A\left(hv - E_g\right)^{\frac{1}{2}} \qquad 5$$

Where A and hv are the photon energy. Urbach energy (E_U) quantifies the static, dynamic disorder resulting from electron-phonon scattering as well as the structural disorder that causes localized exponential-tail states. E_U is estimated below the absorption region (Eg) by equation 6. [15]

$$\ln(\alpha) = \ln(\alpha_0) + \left(\frac{hv}{E_U}\right) \qquad 6$$

where α_0 is a constant.

VPS-300 Biologic potentiostat was used to perform the electrochemical characterization. It used a three-electrode configuration: Ag/AgCl (sat) as the reference electrode, the Cu_2O films as the working electrode, and a platinum counter electrode. Staircase potentio electrochemical impedance spectroscopy (SPEIS) was performed to measure the flat band potential (V_{FB}). It was measured in dark conditions using an electrolyte of 0.1 M $NaCH_3COO$ solution (pH = 7.0) purged with N_2, a frequency of 10 kHz, and the cathodic sweep in the range of -0.5 to 0.5 V (Ag/AgCl) with an amplitude of 25 mV. The E_{FB} values were calculated using the Mott-Schottky equation (Eq. 7) [16]:

$$\frac{1}{C^2} = \frac{2}{\varepsilon\varepsilon_0 A^2 e N_a}\left(V - E_{FB} - \frac{k_B T}{e}\right) \qquad 7$$

where ε is the relative dielectric constant of Cu_2O (7.6); A is the area (cm^2), C is the capacitance (F), V is the applied potential, e is the electron charge (1.602×10^{-19} C); ε_0 is the permittivity of vacuum (8.854×10^{-12} F m^{-1}); k_B is the Boltzmann constant (1.381×10^{-23} JK^{-1}); N_a is the acceptor concentration (cm^{-3}), and T is the absolute temperature (298 K) [17]. The E_{FB} was calculated by the interception of the linear fitting in the Mott-Schottky plot with the x-axis, $1/C^2$ as a function of the applied potential (V). N_a was estimated from the slope (*S*) of the linear fitting of the Mott-Schottky equation (Equation 8).

$$N_a = \frac{2}{\varepsilon\varepsilon_0 A^2 e S} \qquad 8$$

The photoelectrochemical characterization was performed by a cathodic sweep from 0.0 to -0.6 V (Ag/AgCl), the scan rate was 5 $mVs^{-1}$and using 0.5 M $NaSO_4$ as electrolyte solution (pH = 7.0) purged with N_2. A 50 W JDR halogen lamp was used as a light source calibrated in distance to achieve AM 1.5G

conditions. To allow the complete passage of the visible light a reactor with a quartz window was used.

IV RESULTS

Figure 1 shows the XRD patterns of the thin films deposited, in all cases, it can be observed the planes (110), (111), (200), and (220) of the cuprite phase (PDF-03-065-3288). The increase in the number of deposits promotes the increase in thickness of the film since the intensity of the peaks of the FTO substrates decreases considerably. Besides, it is notorious for a change in the preferential orientation from the plane (111) to (200) with the increase in thickness (Table 1), which is characteristic of this process [3].

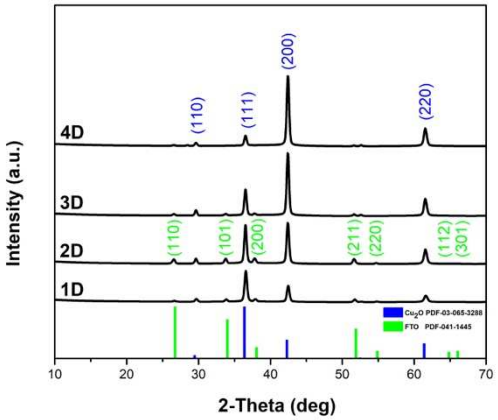

Figure 1: XRD spectra of Cu_2O thin films deposited

The increase in the number of deposits promotes the increase in thickness, which also provokes an increase in the crystallite size (D) and lattice constant ***a*** (Table 1), a condition that has been observed previously in materials deposited by the CBD technique [18], since thicker films have less defect concentration and in consequence bigger size and finer boundaries [12]. The values of texture coefficient of the plane (111) and (200) show the change with more clarity of the preferential orientation, this condition has previously been reported and promotes the increase of resistivity [3].

Table 1: D= crystallite size, FWHM= Full Width at Half Maximum, ***a*** lattice constant, t= thickness, and Tc = texture coefficient (The most intense XRD peak of each film was selected for the estimation of D and ***a*** values).

Deposit	D, nm	FWHM (111), deg	FWHM (200), deg	***a***, Å	t, nm	Tc (111)	Tc (200)
1D	22.6	0.3872	0.3869	4.254	390	0.8	1.21
2D	23.6	0.3623	0.3765	4.261	830	0.5	1.55
3D	25.3	0.3602	0.3515	4.261	1700	0.28	1.95
4D	25.0	0.3719	0.356	4.261	1900	0.12	2.43

The transmittance recorded of the films is presented in figure 2. The increase in the number of deposits promotes the reduction of the transmittance and a decrease in the band gap leading to a redshift, mainly due to the increase in thickness (Table 2) [18]. While the number of constructive interferences increases because of the increase in thickness, the small amplitude of the interferences is related to the rough appearance of the film surface [19,20].

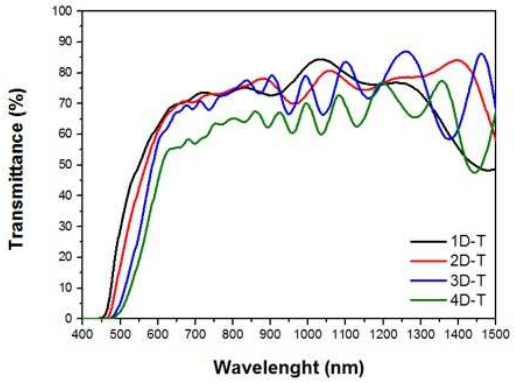

.

Figure 2: Transmittance of Cu_2O thin films deposited

All thin films present a great absorption coefficient ($10^5 cm^{-1}$) in the absorption region (< 460 nm), which reduces with the increase in the number of deposits (Figure 3). Also, a redshift around 460 nm can be observed in agreement with the transmittance and showing a decrease in the band gap (Table 2).

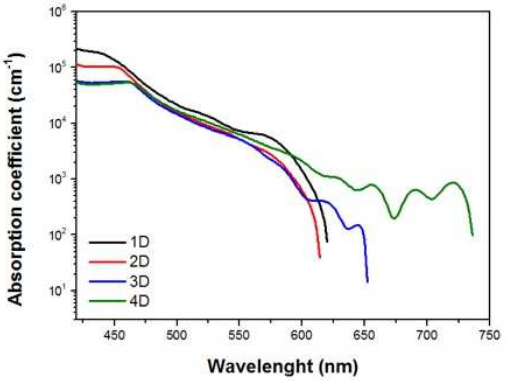

Figure 3: Absorption coefficient of Cu_2O thin films deposited

The FE-SEM figures of the thin films are presented in figure 4. A drastic change in morphology with the increase in the number of deposits can be observed. The 1D film appearance is a well-defined morphology with a particle size bigger than 300 nm. The increase in the number of deposits promotes a loss of well-defined morphology and an increase in particle size (> 600 nm), a condition that we have previously observed for thick films when using a large amount of TEA [3]. However, in the 4D film, it can be observed a slight increase in the particle size and the appearance of new even smaller particles, a condition that is coincident with the structural parameters in table 1, which is related to the low growth of the thickness from deposit 3 to 4, as there was a low growth during these last 4 hours of heating, this energy absorbed by the film during the convection process promotes the fracture of the film. On the other hand, this particle growth and the increase in the XRD peaks without shifting are related to the reduction of structural disorder (E_U) (table 2) due to more controlled growth limiting the presence of defects, which results in an increase in electrical resistivity (Observed as a reduction of carrier density listed in table 2).

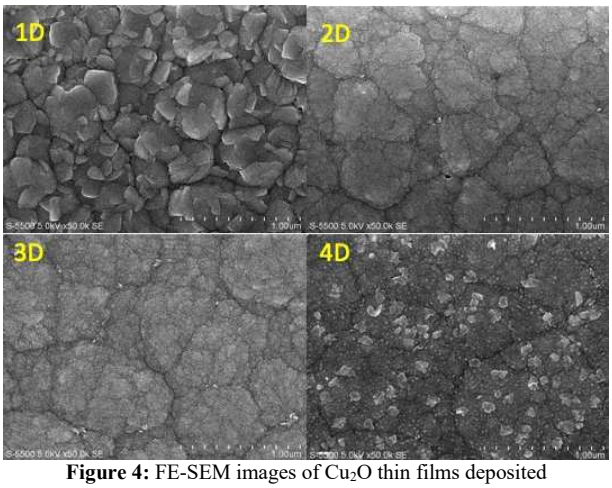

Figure 4: FE-SEM images of Cu_2O thin films deposited

The negative slope in the Mott-Schottky plot means that all films present a p-type semiconductor behavior (Figure 5) [17]. The flat band potential of the Cu_2O thin films presents a shift to higher potentials with the increase in the number of deposits, which is related to the increase in thickness and the decrease of structural disorder (Measured as Urbach energy – Table 2) [21,22] promoting the creation of surface states at the interface with the electrolyte, pinning the Fermi level [17]. These E_{FB} values recorded range from 0.0 to 0.34 V and show that the films can work as photocathodes for hydrogen production by assuming E_{FB} is equal to the valence band (VB) and adding the band gap to estimate the conduction band (CB) [23], as can be seen in figure 6.

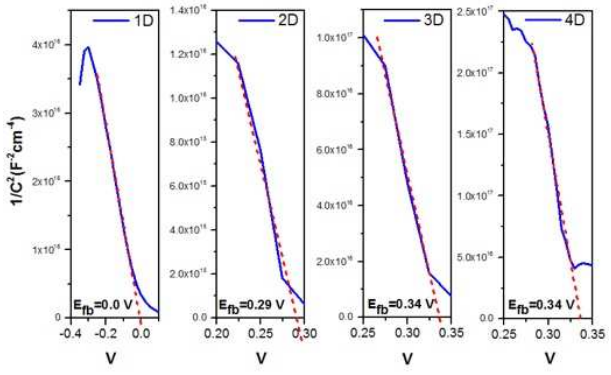

Figure 5: Flat band potential of Cu_2O thin films deposited

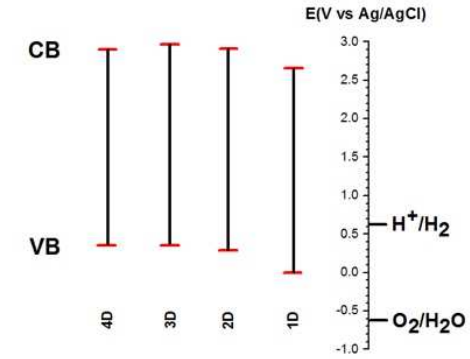

Figure 6: Band alignment of Cu_2O thin films for hydrogen production

Figure 7 presents the photocurrent recorded by the films applying a cathodic sweep potential while a lamp calibrated (AM 1.5) lights on and off. The best performance is observed in the 1D and 4D films, which is explained in the case of 1D due to it being the most conductive and the thinnest (The one with the highest carrier density), which limits the recombination process due to higher electrical transport through less thickness, enhancing the photoresponse. In the case of 4D, although it is the most resistive, it is also the thickest and consequently the one which absorbs more light (Besides, estimating the lowest band gap and therefore the one with the highest photogeneration). While 2D and 3D have a lower performance since competition is established between light absorption and the ability to transport photogenerated charges. All films present problems of charge transport due to the transient current observed in the lighting on/off [24], showing the high resistivity of the material. Table 2 presents the values of E_U and Na, which decrease as the number of deposits increases leading to an increment in the resistivity, showing the effect that structural defects increase the resistivity. Besides, this increase in resistivity is related to the increase in the thickness of the film as we have previously reported [3,25]. These values of E_{FB} and Na are in the range of values reported by similar studies [6,25].

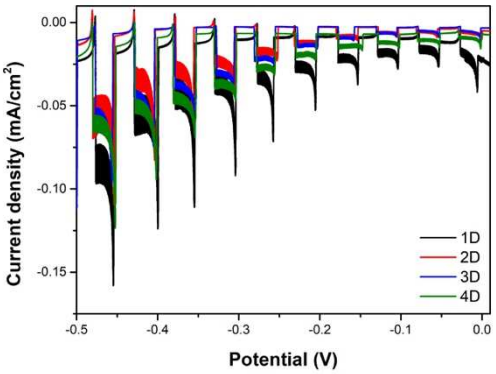

Figure 7: Photocurrent of Cu_2O thin films deposited

Table 2: Optical and electrochemical parameters: Eg= band gap, E_U= Urbach energy, E_{FB}= Flat band potential, and Na= carrier density.

Deposit	Eg, eV	E_U, meV	E_{FB}, mV	Na, cm^{-3}
1D	2.65	211	0.0	1.38E+14
2D	2.63	208	0.29	9.53E+13
3D	2.58	206	0.34	1.67E+13
4D	2.56	206	0.34	4.61E+12

V CONCLUSIONS:

Cu_2O thin films were deposited by the CBD technique in a sequential mode to increase the thickness of the films. The first three deposits substantially increase the thickness of the film, however, the fourth has a lower growth rate which in turn causes greater changes in the optoelectronic properties. As the thickness increases the thin films lose the well-defined morphology increasing the grain size and changing the preferential orientation from the plane (111) to the (200), increasing the particle size, and reducing the structural disorder (Urbach energy), which promotes the reduction of the carrier density, consequently increasing the resistivity. These conditions provoke that the best photocurrents recorded were in the thinnest and thickest films, which are the most conductive and the one which absorbs more light (Lowest band gap), respectively. According to the photoelectrochemical measurements, all films are suitable for working as photocathodes for hydrogen production. Likewise, the thicknesses achieved are interesting for the development of absorbing films for the development of solar cells, however, the band gap of the material must be reduced.

VI DECLARATION OF COMPETING INTEREST:

The authors declare that they have no known competing financial interests or personal relationships that could have appeared to influence the work reported in this paper

VII ACKNOWLEDGMENT:

Odín Reyes-Vallejo, R. Sánchez-Albores, and F.J. Cano acknowledge CONACYT for the postdoctoral and doctoral fellowships respectively. The authors acknowledge the technical support received from Ing. Oscar Gómez Daza, and MSc Alejandra Garcia Sotelo, for general assistance, Dr. Patricia Altuzar Coello and MSc María Luisa Ramón García for XRD analysis, and Rogelio Morán Elvira for SEM images.

VIII REFERENCES

[1] Nandy, S., Banerjee, A.N., Fortunato, E., &Martins, R.(2013). A Review on Cu_2O and CuI-Based p-Type Semiconducting Transparent Oxide Materials: Promising Candidates for New Generation Oxide Based Electronics. Reviews in Advanced Sciences and Engineering,2,1-32.

[2] Rakhshani, A. E. (1986). Preparation, characteristics and photovoltaic properties of cuprous oxide—a review. *Solid-State Electronics*, *29*(1), 7-17.

[3] Reyes-Vallejo, O., Escorcia-García, J., & Sebastian, P. J. (2022). Effect of complexing agent and deposition time on structural, morphological, optical, and electrical properties of cuprous oxide thin films prepared by chemical bath deposition. Materials Science in Semiconductor Processing, 138, 106242.

[4] Nolan, M., & Elliott, S. D. (2006). The p-type conduction mechanism in Cu 2 O: a first-principles study. *Physical Chemistry Chemical Physics*, *8*(45), 5350-5358.

[5] Minami, T., Nishi, Y., & Miyata, T. (2015). Heterojunction solar cell with 6% efficiency based on an n-type aluminum–gallium–oxide thin film and p-type sodium-doped Cu2O sheet. *Applied Physics Express*, *8*(2), 022301.

[6] Jung, K., Lim, T., Bae, H., Ha, J. S., & Martinez-Morales, A. A. (2019). Cu2O photocathode with faster charge transfer by fully reacted Cu seed layer to enhance the performance of hydrogen evolution in solar water splitting applications. *ChemCatChem*, *11*(17), 4377-4382.

[7] Wu, Y. A., McNulty, I., Liu, C., Lau, K. C., Liu, Q., Paulikas, A. P., ... & Rajh, T. (2019). Facet-dependent active sites of a single Cu2O particle photocatalyst for CO2 reduction to methanol. *Nature Energy*, *4*(11), 957-968.

[8] Dolai, S., Das, S., Hussain, S., Bhar, R., & Pal, A. K. (2017). Cuprous oxide (Cu2O) thin films prepared by reactive dc sputtering technique. *Vacuum*, *141*, 296-306.

[9] Tuama, A. N., Abass, K. H., & Agam, M. A. B. (2021). Efficiency enhancement of nano structured Cu2O: Ag/laser etched silicon-thin films fabricated via vacuum thermal evaporation technique for solar cell application. *Optik*, *247*, 167980.

[10] Shinagawa, T., Ida, Y., Mizuno, K., Watase, S., Watanabe, M., Inaba, M., ... & Izaki, M. (2013). Controllable growth orientation of Ag2O and Cu2O films by electrocrystallization from aqueous solutions. *Crystal growth & design*, *13*(1), 52-58.

[11] Ugalde-Reygadas, M., Moreno-Regino, V. D., Torres-Castanedo, C. G., Bedzyk, M. J., Castanedo-Pérez, R., & Torres-Delgado, G. (2022). Cu2O thin films deposited by spray pyrolysis using diethanolamine and L-ascorbic acid as reducing agents. *Materials Today Communications*, 103999.

[12] Reyes, O., Maldonado, D., Escorcia-García, J., & Sebastian, P. J. (2018). Effect of temperature and pH on direct chemical bath deposition of cuprous oxide thin films. *Journal of Materials Science: Materials in Electronics*, *29*(18), 15535-15545.

[13] Grozdanov, I. (1994). Electroless chemical deposition technique for Cu2O thin films. *Materials Letters*, *19*(5-6), 281-285.

[14] Xu, H., Dong, J., & Chen, C. (2014). One-step chemical bath deposition and photocatalytic activity of Cu2O thin films with orientation and size controlled by a chelating agent. *Materials Chemistry and Physics*, *143*(2), 713-719.

[15] Urbach, F. (1953). The long-wavelength edge of photographic sensitivity and the electronic absorption of solids. *Physical Review*, *92*(5), 1324.

[16] Gelderman, K., Lee, L., & Donne, S. W. (2007). Flat-band potential of a semiconductor: using the Mott–Schottky equation. *Journal of chemical education*, *84*(4), 685.

[17] Kalubowila, K. D. R. N., Jayathileka, K. M. D. C., Kumara, L. S. R., Ohara, K., Kohara, S., Sakata, O., ... & Jayanetti, J. K. D. S. (2019). Effect of bath pH on electronic and morphological properties of electrodeposited Cu2O thin films. *Journal of The Electrochemical Society*, *166*(4), D113.

[18] Göde, F., Gümüş, C., & Zor, M. (2007). Investigations on the physical properties of the polycrystalline ZnS thin films deposited by the chemical bath deposition method. *Journal of Crystal Growth*, *299*(1), 136-141.

[19] Swanepoel, R. (1983). Determination of the thickness and optical constants of amorphous silicon. *Journal of Physics E: Scientific Instruments*, *16*(12), 1214.

[20] Swanepoel, R. (1984). Determination of surface roughness and optical constants of inhomogeneous amorphous silicon films. *Journal of Physics E: Scientific Instruments*, *17*(10), 896.

[21] Hssi, A. A., Atourki, L., Labchir, N., Ouafi, M., Abouabassi, K., Elfanaoui, A., ... & Bouabid, K. (2020). Optical and dielectric properties of electrochemically deposited p-Cu2O films. *Materials Research Express*, *7*(1), 016424.

[22] Reyes-Vallejo, O., Sánchez-Albores, R., Fernández-Madrigal, A., Torres-Arellano, S., & Sebastian, P. J. (2022). Evaluation of hydrogen evolution reaction on chemical bath deposited Cu2O thin films: Effect of copper source and triethanolamine content. *International Journal of Hydrogen Energy*.

[23] Liyanaarachchi, U. S., Fernando, C. A. N., Foo, K. L., Hashim, U., & Maza, M. (2015). Structural and Photoelectrochemical Properties of p-Cu_2O Nano-Surfaces Prepared by Oxidizing Copper Sheets with a Slow Heating Rate Exhibiting the Highest Photocurrent and H_2 Evaluation Rate. *Chinese Journal of Physics*, *53*(2), 143-160.

[24] Dotan, H., Sivula, K., Grätzel, M., Rothschild, A., & Warren, S. C. (2011). Probing the photoelectrochemical properties of hematite (α-Fe 2 O 3) electrodes using hydrogen peroxide as a hole scavenger. *Energy & Environmental Science*, *4*(3), 958-964.

[25] Yang, Y., Han, J., Ning, X., Cao, W., Xu, W., & Guo, L. (2014). Controllable morphology and conductivity of electrodeposited Cu2O thin film: effect of surfactants. *ACS Applied Materials & Interfaces*, *6*(24), 22534-22543.